

Article

Effects of Different Point Defects on the Electronic Properties of III–V $\text{Al}_{0.5}\text{Ga}_{0.5}\text{N}$ Photocathode Nanowires

Yiting Li ¹, Qianglong Fang ¹, Yang Shen ^{1,*}, Shuqin Zhang ¹, Xiaodong Yang ², Lanzhi Ye ³ and Liang Chen ^{1,*}

¹ Institute of Optoelectronics Technology, China Jiliang University, Hangzhou 310018, China; s20040809004@cjlu.edu.cn (Y.L.); qlfang0920@foxmail.com (Q.F.); sqzhang@cjlu.edu.cn (S.Z.)

² Key Laboratory of Ecophysics and Department of Physics, Shihezi University, Shihezi 832003, China; yangxiaodong1209@hotmail.com

³ Department of Urban Lighting, Jinhua Garden Landscape Service Center, Jinhua 321099, China; ylz0502@foxmail.com

* Correspondence: yshen@cjlu.edu.cn (Y.S.); lchen@cjlu.edu.cn (L.C.)

Abstract: $\text{Al}_x\text{Ga}_{1-x}\text{N}$ nanowires are the key materials for next-generation ultraviolet (UV) detectors. However, such devices have a low quantum efficiency caused by the introduction of defects and impurities throughout the preparation process of nanowires. Herein, the effects of different interstitial defects and vacancy defects on the electronic structure of $\text{Al}_{0.5}\text{Ga}_{0.5}\text{N}$ nanowires are investigated using density functional theory calculations. Our results successfully discovered that only the formation of an N interstitial defect is thermally stable. In addition, the introduction of different defects makes the different nanowires exhibit n-type or p-type characteristics. Additionally, different defects lead to a decrease in the conduction band minimum in band structures, which is the major cause for the decrease in work function and increase in electron affinity of $\text{Al}_{0.5}\text{Ga}_{0.5}\text{N}$ nanowires. What is more, the calculation of the partial density of states also proved that the interstitial defects contribute to a re-hybridization of local electron orbitals and then cause more significant movement of the electron density. Our investigations provide theoretical guidance for the pursuit of higher-quantum-efficiency ultraviolet (UV) detectors.

Keywords: $\text{Al}_{0.5}\text{Ga}_{0.5}\text{N}$ nanowires; interstitial defect; vacancy defect; electronic structure



Citation: Li, Y.; Fang, Q.; Shen, Y.; Zhang, S.; Yang, X.; Ye, L.; Chen, L. Effects of Different Point Defects on the Electronic Properties of III–V $\text{Al}_{0.5}\text{Ga}_{0.5}\text{N}$ Photocathode Nanowires. *Processes* **2022**, *10*, 625. <https://doi.org/10.3390/pr10040625>

Academic Editor: Domenico Frattini

Received: 1 March 2022

Accepted: 21 March 2022

Published: 23 March 2022

Publisher's Note: MDPI stays neutral with regard to jurisdictional claims in published maps and institutional affiliations.



Copyright: © 2022 by the authors. Licensee MDPI, Basel, Switzerland. This article is an open access article distributed under the terms and conditions of the Creative Commons Attribution (CC BY) license (<https://creativecommons.org/licenses/by/4.0/>).

1. Introduction

In recent years, III–V semiconductor nanowires have been intensively selected in the realm of optoelectronic devices such as solar cells, photodetectors, lasers, and other nanoscale devices [1–3], owing to their fascinating characteristics [4–7]. Furthermore, the $\text{Al}_x\text{Ga}_{1-x}\text{N}$ nanowire photocathode has become the most promising candidates for ultraviolet (UV) detectors due to its adjustable band gap, high temperature resistance, and high sensitivity. However, the defects and impurities throughout the growth and preparation process are the main factors affecting the quantum efficiency of photocathodes [8–12]. Additionally, numerous experiments have detected the defects and impurities on the surface of nanowires [13–16]. Hemesath et al. investigated the incorporation of Au atoms in Si nanowire and proposed new criteria for the stability of planar defects [13]. Biswas et al. discovered that metal impurities in germanium nanowires could substantially alter their electronic and optical properties [14]. Chen et al. studied the incorporation of metal atoms into silicon nanowires and proposed a dimer-atom-insertion kinetic model to explain the impurity incorporation into nanowires [15]. Álvarez et al. found that in InAs nanowires, the surface properties are intimately related to the formation and reaction of surface point defects [16]. However, the experimental studies cannot correctly quantify the variations in nanostructure around the defects and impurities throughout the material growth process. Fortunately, the first-principles calculation method based on density functional theory (DFT) has emerged as an effective means to solve this problem [17–19]. A large number

of studies have been carried out to analyze the effect of defects on the performance of nanowires by first-principles calculations on the basis of no experiments. For example, Yang et al. found through calculations that the As_{Ga} point defect is highly stable in the As-rich condition, regardless of whether the GaAs nanowires are exposed or hydrogen-passive. At the same time, the existence of As_{Ga} point defects inhibits the p-type doping process of GaAs nanowires [20]. Using first principles, Liao et al. found that C_N point defects are more likely to exist on the surface of GaN NWs, and when the defect is closer to the outer side, the effect on the top of the valence band is greater [21]. Kong et al. analyzed first-principles calculations to demonstrate that N vacancy is more likely to exist at the surface of the GaN nanowires and deteriorate the stability [22]. Liu et al. posited that Zn-doped GaAs nanowire suffer more significant surface defects under the same growth conditions due to lower formation energy [23]. Lu et al. explored the optoelectronic properties of native point on GaN nanowires and found that N_{Ga} substitutional defects are the surface defects with the lowest formation energy [24]. Therefore, it is of great significance to study the effect of defects on the properties of nanowires by first-principles calculations. Nevertheless, there are few investigations into the defects and impurities of the $Al_{0.5}Ga_{0.5}N$ nanowire surface. Therefore, in this study, according to the first-principles calculation method, we investigated the impact of surface defects on the electronic characteristics of $Al_{0.5}Ga_{0.5}N$ nanowires.

Herein, interstitial defects and vacancy defects are considered in this study. In addition, in order to maintain the Al composition, only Ga atom and N atom vacancy defects are discussed in this article. The formation energy, work function, electron affinity, geometric structure, Mulliken charge distribution, energy band, and partial density of states are computed and discussed. This study not only explains the physical mechanism of the effect of defects on the $Al_{0.5}Ga_{0.5}N$ nanowire surface but also provide significant guidance for the preparation of high-performance $Al_xGa_{1-x}N$ nanowire-based photocathodes.

2. Calculation Models and Method

All calculations were operated in the Vienna ab initio Simulation Package (VASP) program [25,26]. The Heyd–Scuseria–Ernzerhof (HSE06) functional was implemented to handle the electronic exchanges [27,28]. Following a thorough convergence test, the high energy cut-off was determined to be 400 eV, the thickness of the surrounding vacuum layer was determined to be 25 Å, and the k-point was determined to be $1 \times 1 \times 4$. The energy change was steady within 10^{-4} eV and the force on each atom was less than 0.01 eV, respectively. The valence electrons included: H: $1s^1$, N: $2s^2 2p^3$, Al: $3s^2 3p^1$, and Ga: $3d^{10} 4s^2 4p^1$.

Initially, the $Al_{0.5}Ga_{0.5}N$ nanowires were established by replacing half of the Ga atoms with Al atoms based on the principle of lowest energy [17]. The top views of different defect structures are shown in Figure 1. Moreover, H atoms were selected to eliminate the influence of dangling bonds [29]. In this paper, the positions of interstitial defects and vacancy defects of $Al_{0.5}Ga_{0.5}N$ nanowires were all constructed in the core layer.

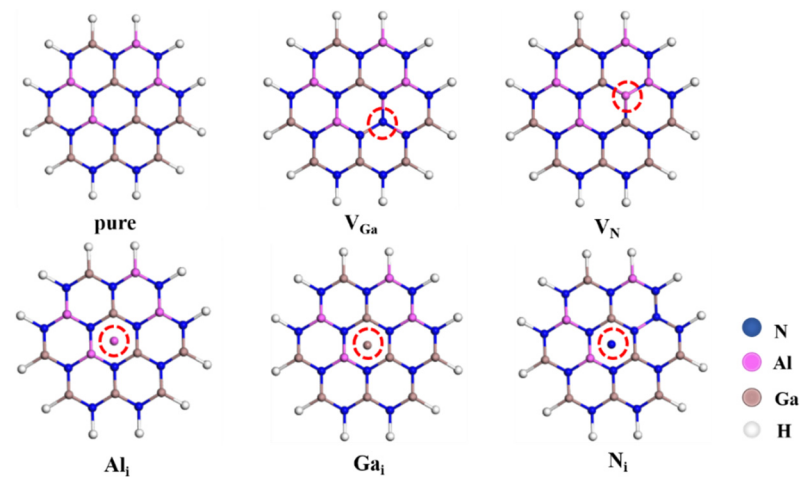


Figure 1. The top views of different defect structures. Pure: no defect; V_{Ga} : Ga vacancy defect; V_N : N vacancy defect; Al_i : Al interstitial defect; Ga_i : Ga interstitial defect; N_i : N interstitial defect.

3. Results and Discussion

There is no doubt that both interstitial defects and vacancy defects affect the stability of the nanowire structure, and the formation energy can be used to assess the stability of $Al_{0.5}Ga_{0.5}N$ nanowires with different defects. What is more, the formation energy can be calculated using the following formula [30]:

$$E_f = E_{defect} - E_{perfect} - \sum_i n_i \mu_i \quad (1)$$

where $E_{perfect}$ and E_{defect} represent the total energy of the structures with and without defects, respectively. n_i represents the number of defect atom, and μ_i represents the chemical potential of the defect atom.

Figure 2a shows the calculated formation energies of different structures. It is clear that compared with the original nanowire structure, the formation process of vacancy defects is an endothermic reaction, which contributes to an unstable nanowire structure. The most difficult to survive is the N atom vacancy defect. Surprisingly, for the formation process of Al and Ga interstitial defects, it is also an endothermic process. However, it is easier to survive than the vacancy defect. Then, for the formation process of N interstitial defects, it is stable owing to negative formation energy, which is consistent with the previous conclusion [24]. According to the previous study [24], the formation energy of the outermost surface defects in the GaN nanowire was about 2.64 eV, while in this study, the formation energy of N interstitial defect at the core position is -3.47 eV. The disparity is mainly due to the differences in Al composition and doping position in the simulated nanowire structures.

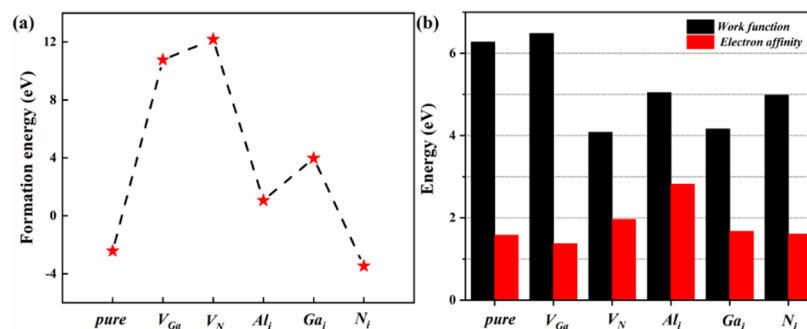


Figure 2. (a) Formation energies of $Al_{0.5}Ga_{0.5}N$ nanowires with different defects. (b) Work function and electron affinity of $Al_{0.5}Ga_{0.5}N$ nanowires with different defects.

In order to quantitatively describe the effect of defects on optoelectronic properties, the work function and electron affinity are firstly calculated in this study. The work function (φ) is the energy difference between the vacuum level (E_{vac}) and the Fermi level (E_f). The electron affinity (χ) is the energy difference between the vacuum level and the conduction band minimum (E_C). The specific formula are as follows [31]:

$$\varphi = E_{vac} - E_f \quad (2)$$

$$\chi = E_{vac} - E_C \quad (3)$$

As is shown in Figure 2b, except for Ga vacancy defects, the introduction of defects contributes to the decrease in surface work function and the slight increase in surface electron affinity. This is mainly attributed to the redistribution of electrons on the nanowire surface caused by the introduction of defects, thereby affecting the transition of photoelectrons. Importantly, it can also be confirmed by the following charge distribution.

On the other hand, the introduction of defects causes changes in the electron density and varying degrees of atom displacements near the defect. Therefore, in order to better understand the effect of introduced defects on the atomic structure and electrons of $\text{Al}_{0.5}\text{Ga}_{0.5}\text{N}$ nanowires, we estimated the bond length, Barder charge distribution, and lattice constant with different defects. The calculated results are shown in Table 1. As calculated, the bond lengths of Ga-N bonds and Al-N bonds in pure $\text{Al}_{0.5}\text{Ga}_{0.5}\text{N}$ nanowires are 1.986 Å and 1.905 Å, respectively, which is similar to the previous study [32]. Furthermore, it is clear in Table 1 that the Al interstitial defects lead to a significant extension of the Al-N bond, extending by 0.601 Å. Next, the interstitial defects have little effect on the Ga-N bond. Additionally, the vacancy defects lead to a decrease in Ga-N bond and Al-N bond. What is more, according to the Barder charge distribution, the initial charge values of Ga atoms, Al atoms, and N atoms in the $\text{Al}_{0.5}\text{Ga}_{0.5}\text{N}$ nanowires without defects are 1.37 eV, 2.37 eV, and -1.89 eV, respectively. Regardless of interstitial defects or vacancy defects, the charge transfer of Al atoms is not obvious, and it is more obvious for Ga atoms and N atoms. Importantly, the N atom vacancy defects greatly reduce the charge of Ga atoms. The introduction of defects also contributes to the reduction in the a-axis and b-axis lattice constant and the increase in c-axis lattice constant, which indicates the closer atomic connections in the horizontal direction of $\text{Al}_{0.5}\text{Ga}_{0.5}\text{N}$ nanowires.

Table 1. Bond length, Barder charge distribution, and lattice constant of $\text{Al}_{0.5}\text{Ga}_{0.5}\text{N}$ nanowires with interstitial defects and vacancy defects.

	Bond Length(Å)		Charge Distribution (e)			Lattice Constant (Å)
	Ga-N	X-N	Ga	Al	X	
Pure	1.986	1.905	+1.37	+2.37	−1.89	a = b = 35.046, c = 5.00
V_{Ga}		1.874	+1.36	+2.357	−1.83	a = b = 35.029, c = 5.11
V_{N}			+1.24	+2.35	−1.90	a = b = 34.826, c = 5.14
Al_i	1.944	2.506	+1.27	+2.34	−1.90	a = b = 35.033, c = 5.00
Ga_i	1.919	1.915	+1.25	+2.376	−1.88	a = b = 35.029, c = 5.15
N_i	1.993	1.905	+1.27	+2.37	−1.72	a = b = 35.027, c = 5.11

In order to further understand the effect of defects on the optoelectrical properties of $\text{Al}_{0.5}\text{Ga}_{0.5}\text{N}$ nanowires, great efforts have been carried out to evaluate the band structures of different models with defects, as shown in Figure 3. It is obvious that the pure $\text{Al}_{0.5}\text{Ga}_{0.5}\text{N}$ nanowire is a direct band gap semiconductor, with a band gap of 5.43 eV. In Figure 3b,c, the appearance of the acceptor energy level can be clearly observed. Compared with the pure $\text{Al}_{0.5}\text{Ga}_{0.5}\text{N}$ nanowire, the band structure of Ga vacancy defect exhibits the p-type characteristic. However, for the N vacancy defect, it contributes to the band structure moving toward lower energy direction and then showing the n-type characteristic. It is mainly attributed to the fact that the vacancy atoms reduce the charge density near the defects. Figure 3d–f show that the interstitial defects introduce impurity energy levels near

the Fermi level, which are represented as donor or acceptor energy levels in the energy band diagram.

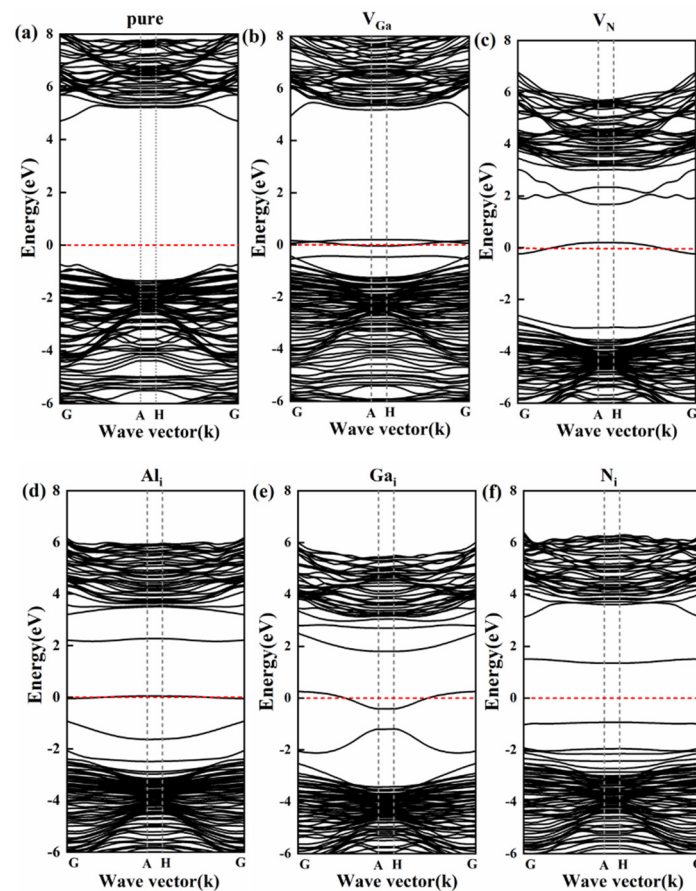


Figure 3. Band structures of different models: (a) pure $\text{Al}_{0.5}\text{Ga}_{0.5}\text{N}$ nanowires, (b) V_{Ga} , (c) V_{N} , (d) Al_i , (e) Ga_i , (f) N_i .

Immediately afterwards, in order to have a deeper understanding of the changes in the band structure, the partial density of states (PDOS) are also considered. Figure 4 shows the PDOS of $\text{Al}_{0.5}\text{Ga}_{0.5}\text{N}$ nanowires with different defects. It can be seen from Figure 4a–c that the interstitial defects introduce a new p-type electronic state near the Fermi level and move toward the lower energy direction, thus passing through the Fermi level and showing n-type characteristics. Among them, the influence caused by Al and Ga interstitial defects is the most obvious. As shown in Figure 4d, due to the lack of N atoms, the density of states of Ga atoms moves towards lower energy as a whole and the total electronic states of Ga atoms decrease. As shown in Figure 4e, due to the lack of Ga atoms in the core position, the peak value of the total electronic states of N atoms has been reduced. Meanwhile, the electronic state of the N atom at the Fermi level is no longer zero and has certain p-type structural characteristics.

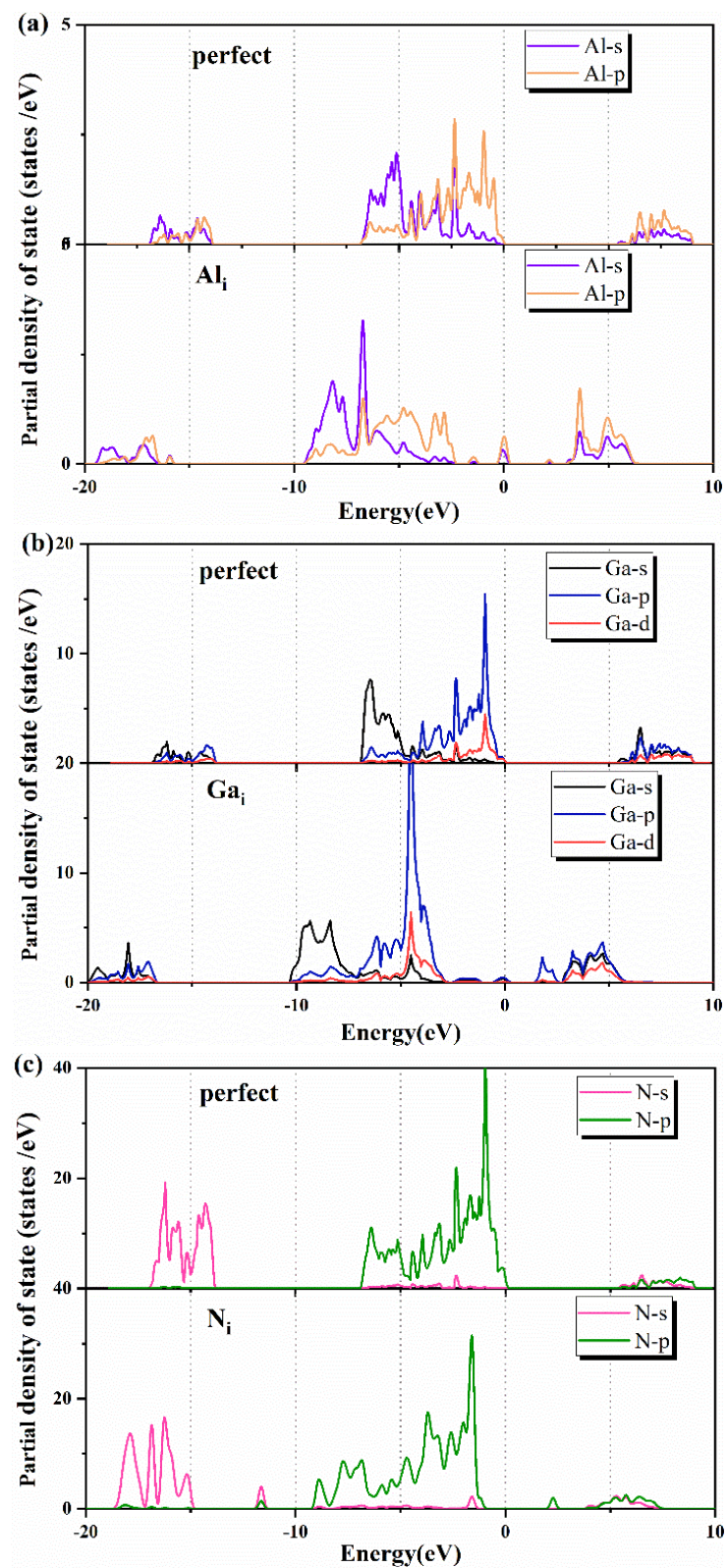


Figure 4. Cont.

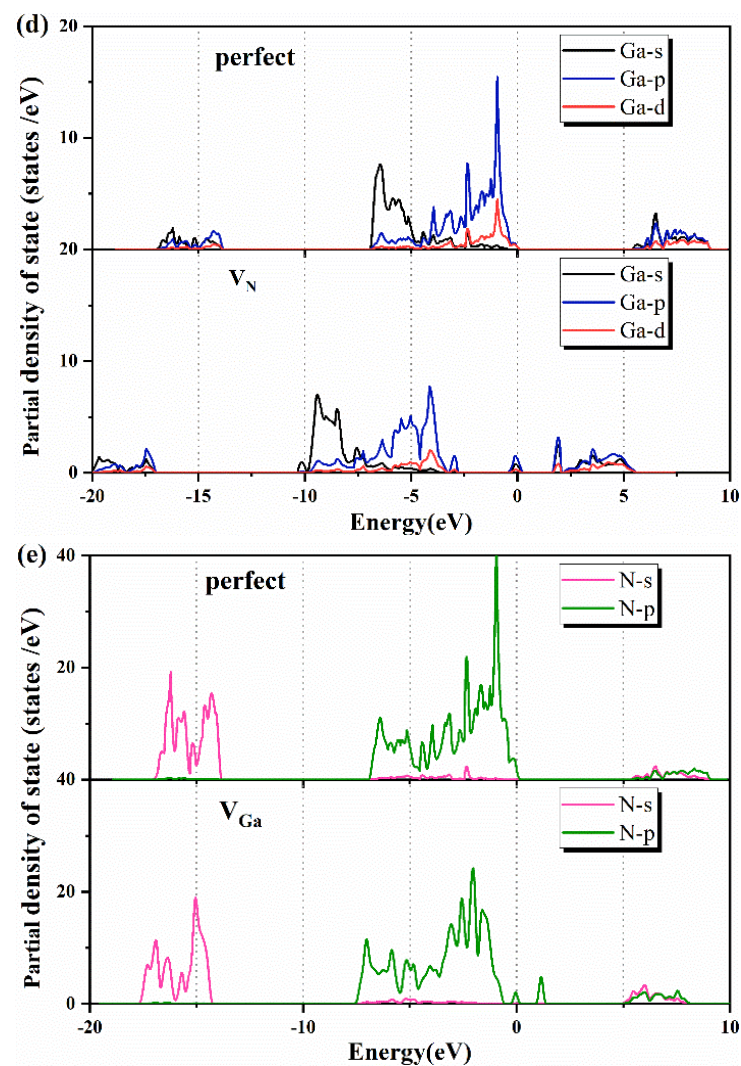


Figure 4. Partial density of states (PDOS) of different defect structures: (a) Al_i , (b) Ga_i , (c) N_i , (d) V_N , (e) V_Ga .

4. Conclusions

In summary, based on the first-principles calculation method, we have investigated the effects of interstitial defects and vacancy defects on the electronic structure of $\text{Al}_{0.5}\text{Ga}_{0.5}\text{N}$ nanowires. From the perspective of formation energy, only the N interstitial defect is an exothermic reaction, which contributes to a thermally stable nanowire structure. In $\text{Al}_{0.5}\text{Ga}_{0.5}\text{N}$ nanowire, interstitial defects are more likely to stably exist than vacancy defects. In addition, except for the Ga vacancy defect, other impurity types cause the work function of the nanowire surface to decrease and the electron affinity to increase. This is mainly due to the decrease in the conduction band minimum in band structures caused by the introduction of defects. Furthermore, the introduction of defects cause changes in the electron density and varying degrees of atom displacements near the defects. In others, the introduction of different defects leads to new donor or acceptor energy levels near the Fermi level in the band structures, making the different nanowires exhibit n-type or p-type characteristics. Overall, this research aims to reveal the effect of different defects on the electronic properties of $\text{Al}_{0.5}\text{Ga}_{0.5}\text{N}$ nanowires, and to provide systematical guidance for subsequent experimental preparation.

Author Contributions: Methodology, Q.F.; software, X.Y. and L.Y.; validation, S.Z.; formal analysis, Y.L.; investigation, X.Y.; resources, Q.F. and S.Z.; writing—original draft preparation, Y.L.; writing—

review and editing, Y.S.; visualization, L.Y.; supervision, Y.S.; project administration, L.C.; funding acquisition, Y.S. All authors have read and agreed to the published version of the manuscript.

Funding: This work was supported by the National Natural Science Foundation of China (Grant Nos. 62,004,183 and 62075205), Natural Science Foundation of Zhejiang Province (Grant Nos. LQ21F050011 and LZ20F050001) and the Fundamental Research Funds for the Provincial Universities of Zhejiang (Grant Nos. 2020YW48, 2021YW11 and 2021YW87).

Institutional Review Board Statement: Not applicable.

Informed Consent Statement: Not applicable.

Data Availability Statement: Not applicable.

Acknowledgments: We thanks Jianguo Wan from Nanjing University for providing us with first-principles computational resources.

Conflicts of Interest: The authors declare no conflict of interest.

References

1. Mizuno, S. Acoustic Phonon Modes and Phononic Bandgaps in GaN/AlN Nanowire Superlattices. *Nanoscale Res. Lett.* **2012**, *7*, 479. [[CrossRef](#)] [[PubMed](#)]
2. Jayaprakash, R.; Ajagunna, D.; Germanis, S.; Androulidaki, M.; Tsagaraki, K.; Georgakilas, A.; Pelekanos, N.T. Extraction of Absorption Coefficients from as-Grown GaN Nanowires on Opaque Substrates Using All-Optical Method. *Opt. Express* **2014**, *22*, 19555–19566. [[CrossRef](#)]
3. Nam, C.-Y.; Jaroenapibal, P.; Tham, D.; Luzzi, D.E.; Evoy, S.; Fischer, J.E. Diameter-Dependent Electromechanical Properties of GaN Nanowires. *Nano Lett.* **2006**, *6*, 153–158. [[CrossRef](#)] [[PubMed](#)]
4. Kim, S.S.; Park, J.Y.; Choi, S.W.; Kim, H.S.; Na, H.G.; Yang, J.C.; Lee, C.; Kim, H.W. Room Temperature Sensing Properties of Networked GaN Nanowire Sensors to Hydrogen Enhanced by the Ga₂Pd₅ Nanodot Functionalization. *Int. J. Hydrog. Energy* **2011**, *36*, 2313–2319. [[CrossRef](#)]
5. Sergent, S.; Damilano, B.; Vézian, S.; Chenot, S.; Tsuchizawa, T.; Notomi, M. Lasing Up to 380 K in a Sublimated GaN Nanowire. *Appl. Phys. Lett.* **2020**, *116*, 223101. [[CrossRef](#)]
6. Routray, S.; Lenka, T. Performance Analysis of Nanodisk and Core/Shell/Shell-Nanowire Type III-Nitride Heterojunction Solar Cell for Efficient Energy Harvesting. *Superlattices Microstruct.* **2017**, *111*, 776–782. [[CrossRef](#)]
7. Mao, S.; Liu, Y.; Li, P.; Meng, X. Fabrication and Comparative Study of Vertically Grown and Horizontally-Dispersed Fully Nanowire-Based Photodetectors. *Appl. Surf. Sci.* **2015**, *359*, 496–499. [[CrossRef](#)]
8. Memisevic, E.; Hellenbrand, M.; Lind, E.; Persson, A.R.; Sant, S.; Schenk, A.; Svensson, J.; Wallenberg, R.; Wernersson, L.-E. Individual Defects in InAs/InGaAsSb/GaSb Nanowire Tunnel Field-Effect Transistors Operating below 60 mV/Decade. *Nano Lett.* **2017**, *17*, 4373–4380. [[CrossRef](#)]
9. Roy, A.; Mead, J.; Wang, S.; Huang, H. Effects of Surface Defects on the Mechanical Properties of ZnO Nanowires. *Sci. Rep.* **2017**, *7*, 9547. [[CrossRef](#)]
10. Wang, J.; Wang, J.G.; Qin, X.; Wang, Y.; You, Z.; Liu, H.; Shao, M. Superfine MnO₂ Nanowires with Rich Defects toward Boosted Zinc Ion Storage Performance. *ACS Appl. Mater. Interfaces* **2020**, *12*, 34487–35766. [[CrossRef](#)]
11. Heo, J.; Cho, K.-H.; Jain, P.K. Motion of Defects in Ion-Conducting Nanowires. *Nano Lett.* **2020**, *21*, 556–561. [[CrossRef](#)] [[PubMed](#)]
12. Dai, S.; Zhao, J.; He, M.-R.; Wang, X.; Wan, J.; Shan, Z.; Zhu, J. Elastic Properties of GaN Nanowires: Revealing the Influence of Planar Defects on Young's Modulus at Nanoscale. *Nano Lett.* **2014**, *15*, 8–15. [[CrossRef](#)] [[PubMed](#)]
13. Hemesath, E.R.; Schreiber, D.K.; Gulsoy, E.B.; Kisielowski, C.F.; Petford-Long, A.K.; Voorhees, P.W.; Lauhon, L.J. Catalyst Incorporation at Defects during Nanowire Growth. *Nano Lett.* **2011**, *12*, 167–171. [[CrossRef](#)] [[PubMed](#)]
14. Biswas, S.; Barth, S.; Holmes, J.D. Inducing Imperfections in Germanium Nanowires. *Nano Res.* **2017**, *10*, 1510–1523. [[CrossRef](#)]
15. Chen, W.; Yu, L.; Misra, S.; Fan, Z.; Pareige, P.; Patriarche, G.; Bouchoule, S. Incorporation and Redistribution of Impurities into Silicon Nanowires during Metal-Particle-Assisted Growth. *Nat. Commun.* **2014**, *5*, 4134. [[CrossRef](#)]
16. Alvarez, A.D.; Peric, N.; Vergel, N.A.F.; Nys, J.-P.; Berthe, M.; Patriarche, G.; Harmand, J.-C.; Caroff, P.; Plissard, S.; Ebert, P.; et al. Importance of Point Defect Reactions for the Atomic-Scale Roughness of III–V Nanowire Sidewalls. *Nanotechnology* **2019**, *30*, 324002. [[CrossRef](#)]
17. Xia, S.; Liu, L.; Kong, Y.; Wang, H.; Wang, M. Study of Cs Adsorption on (100) Surface of [1]-Oriented GaN Nanowires: A First Principle Research. *Appl. Surf. Sci.* **2016**, *387*, 1110–1115. [[CrossRef](#)]
18. Srivastava, M.; Srivastava, A. Electron Transport in CO₂ Adsorbed ZnO Nanowire: DFT Study. *Chem. Phys. Lett.* **2019**, *729*, 17–23. [[CrossRef](#)]
19. Tan, T.L.; Ng, M.-F. Computational Screening for Effective Ge_{1–x}Si_x Nanowire Photocatalyst. *Phys. Chem. Chem. Phys.* **2015**, *17*, 20391–20397. [[CrossRef](#)]
20. Shu, H.; Yang, X.; Liang, P.; Cao, D.; Chen, X. Impact of Surface Point Defects on Electronic Properties and P-Type Doping of GaAs Nanowires. *J. Phys. Chem. C* **2016**, *120*, 22088–22095. [[CrossRef](#)]

21. Liao, H.; Li, J.; Wei, T.; Wen, P.; Li, M.; Hu, X. First-Principles Study of CN point defects on sidewall surface of [0 0 0 1]-oriented GaN nanowires. *Appl. Surf. Sci.* **2018**, *467*, 293–297. [[CrossRef](#)]
22. Kong, Y.; Liu, L.; Xia, S.; Wang, H.; Wang, M. Research on Optoelectronic Properties of GaN Nanowires with N Vacancy. *Comput. Theor. Chem.* **2016**, *1092*, 19–24. [[CrossRef](#)]
23. Liu, L.; Diao, Y.; Xia, S. Intrinsic Point Defects in Pristine and Zn-Doped GaAs Nanowire Surfaces: A First-Principles Investigation. *Appl. Surf. Sci.* **2020**, *514*, 145906. [[CrossRef](#)]
24. Lu, F.; Liu, L.; Tian, J. Optoelectronic Properties Exploration of Native Point Defects on GaN Nanowires. *Appl. Surf. Sci.* **2021**, *565*, 150600. [[CrossRef](#)]
25. Hafner, J. Materials Simulations Using VASP—A Quantum Perspective to Materials Science. *Comput. Phys. Commun.* **2007**, *177*, 6–13. [[CrossRef](#)]
26. Hafner, J. ChemInform Abstract: Ab-Initio Simulations of Materials Using VASP: Density-functional Theory and Beyond. *ChemInform* **2008**, *39*, 2044–2078. [[CrossRef](#)]
27. Perdew, J.P.; Burke, K.; Ernzerhof, M. Generalized Gradient Approximation Made Simple. *Phys. Rev. Lett.* **1996**, *77*, 3865. [[CrossRef](#)]
28. Dinh, P.M.; Messud, J.; Reinhard, P.G.; Suraud, E. Self-Interaction Correction in a Simple Structure. *Phys. Lett. A* **2008**, *372*, 5598–5602. [[CrossRef](#)]
29. Wang, D.; Tang, L.-M. Electronic Structure and Magnetism of Doped Wurtzite InSb Nanowire. *J. Phys. D Appl. Phys.* **2016**, *49*, 175303. [[CrossRef](#)]
30. Wang, Z.; Li, J.; Gao, F.; Weber, W.J. Defects in Gallium Nitride Nanowires: First Principles Calculations. *J. Appl. Phys.* **2010**, *108*, 044305. [[CrossRef](#)]
31. Zou, J.; Chang, B.; Yang, Z.; Zhang, Y.; Qiao, J. Evolution of Surface Potential Barrier for Negative-Electron-Affinity GaAs Photo-Cathodes. *J. Appl. Phys.* **2019**, *105*, 013714. [[CrossRef](#)]
32. Yang, M.; Fu, X.; Guo, J.; Rao, W. Electronic Structure and Optical Properties of Al_{0.25}Ga_{0.75}N with Point Defects and Mg-Defect Complexes. *Opt. Quantum Electron.* **2018**, *50*, 60. [[CrossRef](#)]